Preferred citation: R. Bollström and M. Toivakka. Paper substrate for printed functionality. In **Advances in Pulp and Paper Research, Cambridge 2013**, *Trans. of the XVth Fund. Res. Symp. Cambridge, 2013*, (S.J. I'Anson, ed.), pp 945–966, FRC, Manchester, 2018. DOI: 10.15376/frc.2013.2.945.

PAPER SUBSTRATE FOR PRINTED FUNCTIONALITY

Roger Bollström and Martti Toivakka

Laboratory of Paper Coating and Converting, Centre for Functional Materials
Åbo Akademi University

ABSTRACT

Requirements for paper to be used as substrate for printed functionality were investigated. A recyclable, multilayer-coated paper substrate that combines adequate barrier and printability properties for printed electronics and sensor applications was developed. In this multilayer structure, a thin top-coating consisting of mineral pigments is coated on top of a dispersion-coated barrier layer. The top-coating provides well-controlled sorption properties through controlled thickness and porosity, thus enabling optimizing the printability of functional materials. The optimum barrier layer structure was investigated by studying the influence of latex type and amount in blends with different size and shape factor kaolin pigments. Highly aligned high shape factor kaolin improved barrier properties in general, but was found especially useful against organic solvents, which may degrade the latex. Dimensional stability and its influence on substrate surface properties as well as on functionality of conductive tracks were studied by exposure to high/low humidity cycles. The barrier layer of the multilayer coated paper reduced the dimensional changes and surface roughness increase caused by humidity and helped maintain the conductivity of printed tracks. As proof of concept functional devices, hygroscopic insulator field effect transistors were printed on the multi-layer curtain coated paper using a custom-built roll-to-roll hybrid printer.

1 INTRODUCTION

Mass-produced paper electronics (large area organic printed electronics on paper-based substrates, "throw-away electronics") has the potential to introduce the use of flexible electronic applications in everyday life. While paper manufacturing and printing have a long history, they were not developed with electronic applications in mind. Low-cost and recyclable paper substrates are being considered for various novel, value-added printed applications outside the conventional graphical arts industry [1, 2, 3, 4, 5, 6]. Electronic devices such as transistors, capacitors, radio frequency identification (RFID) antennas and batteries have been fabricated on paper or paper-like substrates by using functional inks containing e.g. conducting and semiconducting materials, such as silver, organic polymers as well as carbon nanotubes [7, 8, 9, 10, 11, 12, 5]. Organic photodiodes and photovoltaic cells, electronic paper displays, foldable thermochromic displays and high-performance organic thin film transistor arrays on paper have also been demonstrated [13, 14, 15]. Recently also sensors for analysis of ionic concentration, analysis of modified atmosphere conditions, as well as sensors for use in diagnostics applications, have been manufactured by printing on paper [16, 17, 18, 19, 20, 21]. Sufficient surface smoothness of substrate is necessary for many printed electronics applications, especially for multilayer devices, where a single peak may cause short circuits and render the device inoperable [22, 23, 24, 25]. By adjusting the substrate surface energy relative to the surface tension of the ink, the spreading and adhesion of the functional materials can be controlled. Penetration of ink components into the substrate can be eliminated by use of barrier coating [26, 24, 27, 28, 29].

Poor dimensional stability, which can cause cracks and disconnects in printed tracks, has been considered a challenge when using fiber-based materials. Humidity and temperature variations have a strong impact on the fibers, the bindings between them as well as the size and length of them [30, 31, 32]. Transferring materials onto the substrate, by use of coating or printing methods, involves use of solvents combined with harsh drying methods, all having a strong impact on the dimensional stability of the fiber network. From the end product point of view, maintaining functionality in varying weather and temperature conditions is important. One way to reduce the problems associated with the fiber network expansion is to apply a barrier layer on substrate surface to limit the solvent and humidity penetration. Various types of dispersion polymers, commonly known as latexes, either coated as pure or in combination with mineral pigments can be used for improving barrier properties against humidity, grease or solvent penetration [33, 34, 35].

This work focuses on understanding the requirements for paper when used as substrate for printed functionality. This article compiles results from several separately published articles and summarizes important findings. The interactions between coated paper and setting of different functional inks are studied. Furthermore the requirements for a paper to withstand functional processing and storage in harsh conditions are investigated. As proof of concept a roll-to-roll printed transistor is demonstrated on the multilayer coated paper.

2 MATERIALS AND METHODS

The details of the multi-layer coated paper-based substrates that were used in the current work are reported elsewhere [36, 37, 29]. The differences between the substrates are mainly related to the thickness and the formulation of the top-coating, which controls the printability of the functional inks. Regarding the barrier layer formulation, the main differences are pigment volume concentration (PVC), pigment aspect ratio, binder chemistry as well as layer thickness [38, 35]. For printing of silver electrodes, two commercial conductive inks were used; Suntronic 5603 Ag nano particle inkjet silver ink, and Creative Materials 125–06 micron size particle flexography silver ink. Regioregular poly(3-hexylthiophene) (P3HT) was used as the semiconductor and poly(4-vinylphenol) (PVP) as insulator. PEDOT:PSS (H.C. Starck) organic conductive polymer was used for the gate electrode in the printed transistor. Printings were carried out either in batch process (DMP-2831, Dimatix-Fujifilm Inc.) or with a custom-built roll-to-roll hybrid printer. In roll-to-roll processing the printing speed was 10 m/min, the web width 100 mm and eight 500 W infrared sintering units were mounted online. The flexographic silver printing (including source and drain electrodes for the transistor) were carried out using an ASAHI DSH® (Shore A 69º) photopolymer printing plate with a ceramic anilox cylinder (Cheshire Engraving Cervices Ltd., cell angle 60º, line density 120 lines/cm, cell volume of 12 cm^3/m^2). The roll-to-roll inkjet printhead fed by a custom-built ink-feed setup is a 128 nozzle and 80 pl drop volume Xaar operated by Imaje 4400 controller and software.

3 RESULTS AND DISCUSSION

3.1 Paper structure

It is not possible to define a single paper concept that could be considered a "paper for printed electronics." The suitability of the paper depends on the functional materials deposited on it to fabricate the targeted device. However, there are some general properties, which either are a prerequisite for functioning of a printed device, or which improve the performance of it. These include surface smoothness, barrier properties to maintain the functional materials on paper surface, and print definition. Considering the above, the authors have developed a multilayer-coated, paper-based substrate concept that is suitable for printed electronics and functionality [39, 36, 29]. In this multilayer structure, shown in Figure 1, a thin top-coating consisting of mineral pigments is coated on top of a dispersion-coated barrier layer. The top-coating provides well-controlled ink spreading and sorption properties through controlled thickness and porosity, thus enabling optimizing the printability of functional materials (section 3.3). The penetration of ink solvents and functional materials stops at the barrier layer (section 3.2), which not only improves the performance of the functional material but also eliminates potential fiber swelling and de-bonding that can occur if solvents are allowed to penetrate into the base paper (section 3.4). Additionally, the mineral pigment coating improves the heat stability of the paper enabling online infrared sintering with relatively high temperatures [40]. The multi-layer coated paper under consideration in the current work consists of a pre-coating and a smoothing layer under the barrier layer. Coated fine paper may also be used directly as basepaper, as long a smooth base for the barrier layer is ensured. The top coating layer is thin and smooth (coat weight 0.5–10 g/m^2, layer thickness 0.5–5 µm, root mean square (RMS) surface roughness 55–75 nm) consisting of mineral pigments such as kaolin, calcium carbonate, silica or blends of these. All the materials in the coating structure are chosen in order to maintain the recyclability and sustainability of the substrate. The substrate can be coated in steps, sequentially layer by layer, which requires detailed understanding and tuning of the wetting properties and topography of the barrier layer versus the surface tension of the top-coating [38]. An alternative, cost competitive method for industrial scale production is the curtain

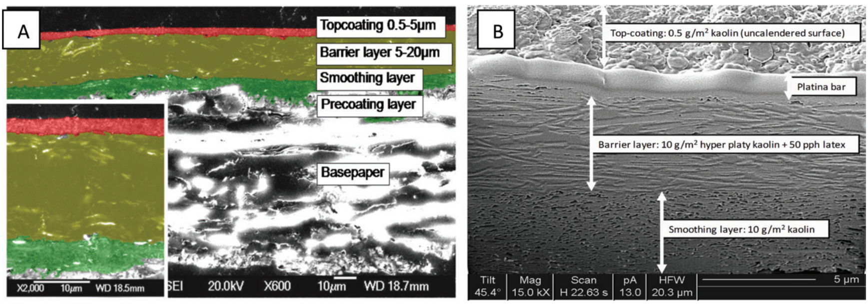

Figure 1. A: Cross-section scanning electron microscope (SEM) image showing the layer structure of the paper substrate: top-coating, barrier layer, smoothing layer, pre-coating and basepaper. Reproduced with permission. Copyright 2009, Elsevier [36]. B: Focused ion beam etched cross-section image. Reproduced with permission. Copyright 2012, Elsevier [29].

coating, which enables simultaneous coating of all the layers in one pass [29, 37, 41, 42, 43].

3.2 Barrier properties

In functional printing and coating, conductive, semi-conductive and insulating materials are usually dissolved in organic solvents such as dichlorobenzene or toluene. Although these liquids are brought into a direct contact with the substrate, the solvents evaporate quite rapidly, suggesting that short term barrier properties might suffice. On the other hand, in throw-away sensor applications, for example for medical use, acidic or basic analytes may be used and the sensoring process might last for several minutes and long term barrier properties are needed [44, 45, 46, 47, 48, 49]. In the multilayer coating structure the barrier layer both controls the absorption of the inks during device fabrication and ensures the end-use function. A simple example of a sorption test for a semiconductor ink, regioregular poly(3-hexylthiophene) (P3HT) dissolved in ortho-dichlorobenzene (DCB), is shown in Figure 2A. The amount of ink applied was the same for each sample (5 µl), and the scanned areas were 25 × 25 mm^2 except for the Mylar® A where an

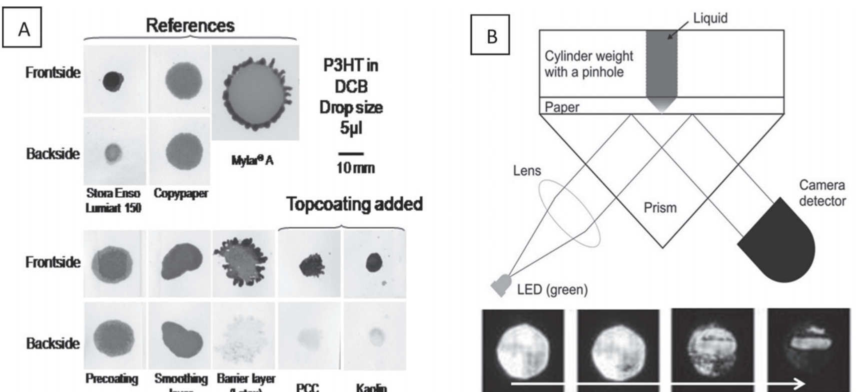

Figure 2. A: A simple barrier test, application of semiconductor ink dissolved in DCB onto different substrates and scanning of the spots from the front and backside of the substrate. A visible spot on the backside indicates solvent and functional ink penetration. Reproduced with permission. Copyright 2009, Elsevier [36]. B: Method for measuring active barrier lifetime, i.e. penetration through the substrate as function of time, via change in effective refractive index at paper-glass prism interface. Reproduced with permission. IOP Publishing. Copyright 2012 [50].

area of 35 × 35 mm^2 was needed because of the excessive droplet spreading. To be able to study in detail the effective barrier properties against solvents, novel barrier measurement methods were developed. A practical method for obtaining the active barrier lifetime is a prism method schematically presented in Figure 2B. The penetration through the substrate is monitored as function of time as changes in the effective refractive index at the prism-paper interface [50].

Dispersion coating has received attention as a production method for barrier coatings, since it has been considered to be more environmentally friendly in comparison to extrusion coating and lamination [51, 52, 53, 34, 33]. Traditional paper- and board-based products, such as those used in packaging, require high barrier properties against gases and liquids. If paper is to be used as a substrate in functional applications, the required barrier properties against solvents and acids need to be understood and developed. The current work aimed at understanding how a dispersion coated barrier layer is optimally built up and how various polymer dispersions and pigments function as a barrier against water vapor as well as against an organic solvent (DCB) and an acid. High (100) (Platy kaolin) and low (30) (Fine kaolin) shape factor pigments were blended with different amounts of styrene-acrylate (SA), styrene-butadiene (SB) and ethylene-acrylate (EA) latex as well as starch. For barrier dispersions, a specific ratio between the pigment and the binder addition levels exists, acting as a threshold level, at which barrier properties change significantly, due to introduction of porosity into barrier layer. For barrier coating, it is of utmost importance to have knowledge of this critical pigment volume concentration (CPVC). The CPVC was determined by measuring light scattering as function of drying time at different pigment addition levels and found to be 55.7% for the platy kaolin and 62.8% for the fine kaolin [53, 54, 55].

Figure 3 shows the influence of high (100) and low (30) shape factor kaolin additions on barrier properties (water vapor transfer rate (WVTR), normalized to 15 μm). In the case of low shape factor kaolin, the improvement in barrier properties is only minimal compared to pure latex (SA). However, the addition of pigments reduces the blocking problem, which occurred for the sticky surface of the pure SA latex and caused defects in rewinding thereby also deteriorating the barrier properties. Addition of high shape factor (100) kaolin however significantly reduces the penetration at both PVC levels when combined with SA latex. The standard deviation of the barrier properties measured from the coatings containing low shape factor kaolin were significantly larger compared to the practically negligible standard deviation of the barrier results obtained from the coatings filled with high shape factor kaolin. This may be a result of nonhomogenous or poor alignment of the particles, as shown in figure 4B.

Figure 5 shows the WVTR for three latexes with different chemistry, filled with high shape factor (100) kaolin. As a reference material to the latexes, starch

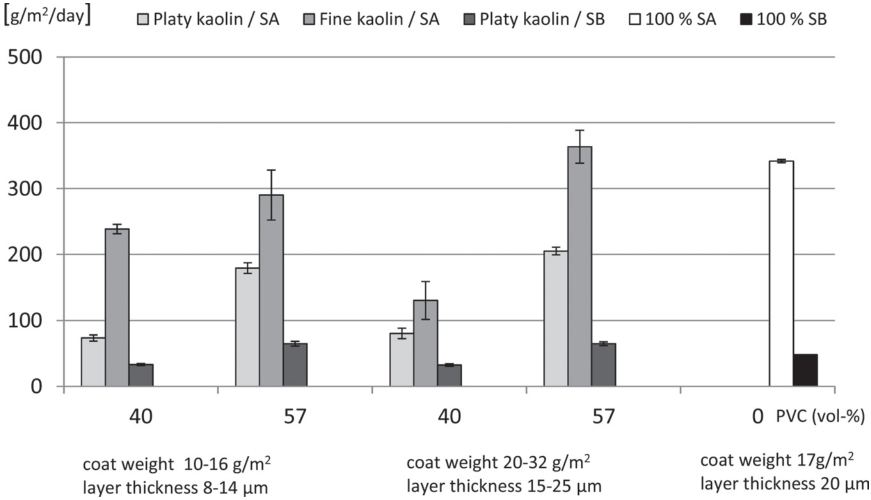

Figure 3. Normalized (15 µm thickness) WVTR at 23ºC and 85% relative humidity (RH) for kaolin with a shape factor of 30 (Fine kaolin) and 100 (Platy kaolin) combined with different amounts of SA and SB latex [35].

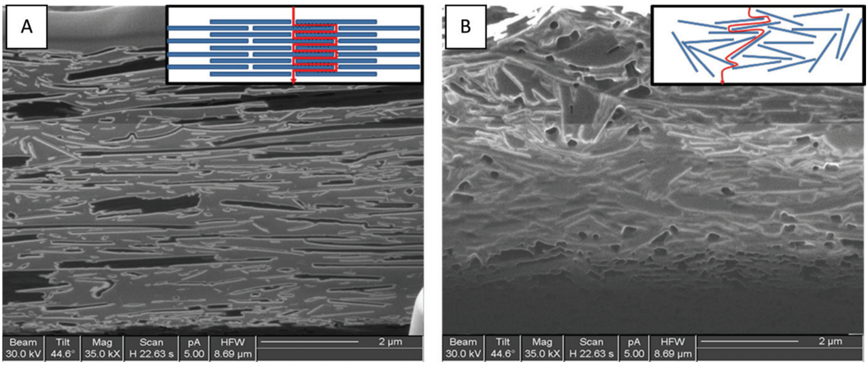

Figure 4. Focused ion beam images showing the alignment of the kaolin particle filled latex barrier layer. A: Highly aligned high shape factor kaolin. B: Poorly aligned low shape factor kaolin. The tortuosity of the structures is shown schematically in the inserted images [35].

was also tested as barrier polymer. The water soluble anionic starch however dissolves resulting in very poor barrier properties against water vapor (note the discontinuous Y-axis scale). Despite the dissolving of the starch, the thicker layer (25 µm) clearly improves the barrier properties compared to the thinner (10 µm),

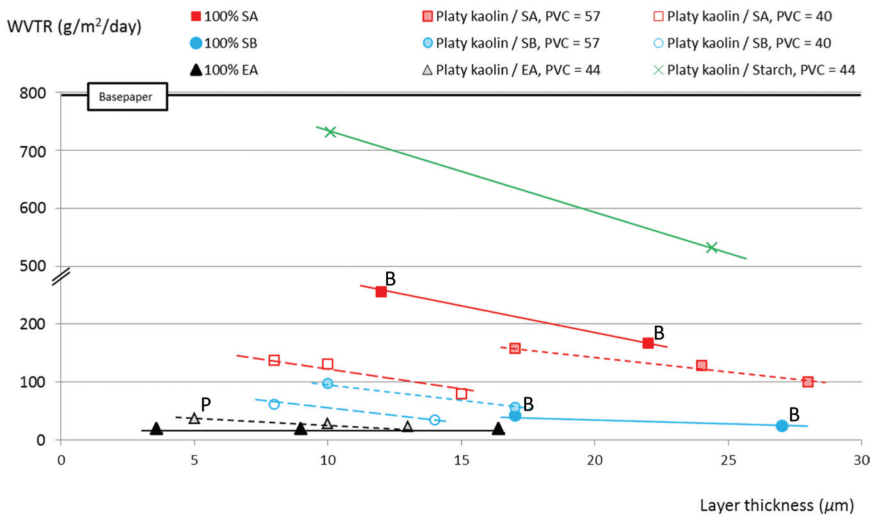

Figure 5. Barrier properties against water vapor (WVTR) at 23ºC and 85% RH as a function of barrier layer thickness. The values are average values of three parallel measurements, with a negligible standard deviation. (B = Tendency for blocking, P = risk for pinholes). Note the discontinuous Y-axis scale.

which is explained by the longer pathway through the tortuous kaolin structure. Regarding the latexes, the most obvious difference can be seen for the styrene acrylate latex where addition of kaolin clearly improves the barrier properties at the same layer thickness, whereas for the styrene butadiene latex the difference is smaller. While the highest barrier properties could be obtained by using pure ethylene acrylic latex, an addition of 44 vol-% kaolin did not significantly weaken the barrier properties against water vapor, which is an economic advantage in commercial applications. The WVTR barrier properties for the basepaper (including precoating and smoothing layer) were 795 g/m^2/day.

In addition to barrier properties against water vapor, barrier properties against liquids directly applied onto the surface of the substrate were measured. These measurements were made in order to mimic a coating or printing operation, or an analysis procedure in a printed functional application [50]. Organic solvents are common as ink vehicles and acids are used as analytes in sensor applications, both requiring barrier properties for varying times. Figure 6 plots the time it takes for ortho-dichlorobenzene (DCB) to penetrate the substrates. As can be seen for all the latexes, the addition of high shape factor kaolin clearly improves the barrier properties. This can be related to the increased tortuosity through the particle filled structure (Figure 4A). The organic solvent dissolves partially the latex but

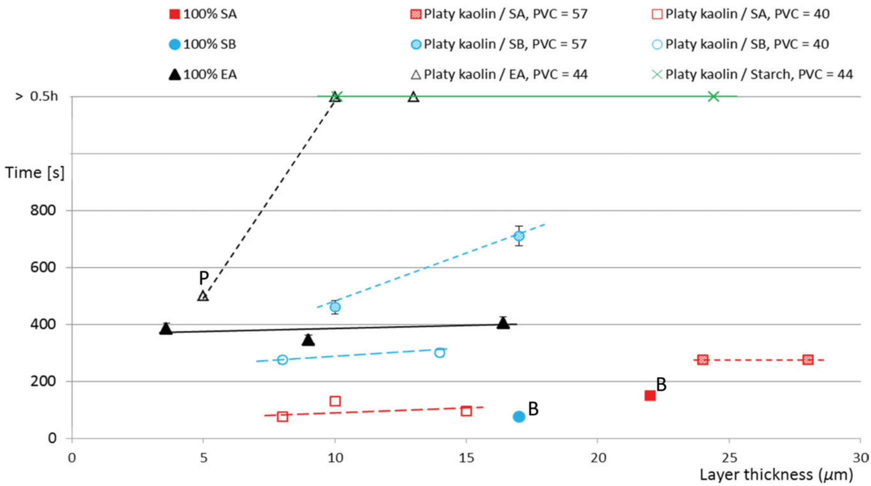

Figure 6. Barrier properties against ortho-dichlorobenzene. The figure shows the time in seconds for the liquid to penetrate the substrate. (B = Tendency for blocking, P = risk for pinholes). Penetration time measured with prism method presented in Figure 2B [50].

the inert high shape factor mineral particles create a long pathway for the solvent to migrate through. DCB, on the contrary to the water vapor, does not dissolve the starch, which as a polar molecule performs well as a barrier against the nonpolar DCB. Figure 6 only plots the short term barrier properties, but for the starch coatings the barrier measurements were extended to three days by addition of DCB to counteract the evaporation. No DCB penetrated the starch based barrier coatings during the three days, indicating the starch is completely insoluble by DCB. Differences in dissolving or degrading of the latexes can also be seen, the styrene-butadiene and styrene-acrylic latexes dissolving most rapidly while the ethylene-acrylic can withstand the organic solvent for longer.

In contrast to the barrier properties against DCB, the pure latexes and the layers with low pigment volume concentration show the best barrier properties against 1M hydrochloric acid (Figure 7). This can be related to voids existing in the layers filled to 57% by pigments, since the critical pigment volume concentration for the platy kaolin was found to be 55.7%. The lower amount of organic material on the surface of these layers can result in a more hydrophilic surface and more complete wetting [35, 38]. In the case of the thin (5 μm) kaolin/ethylene acrylic latex layer the penetration was caused by pinholes. The latexes are all inert against the hydrochloric acid showing no degradation or dissolving tendency as was the case for the organic solvent. The water soluble starch was dissolved immediately

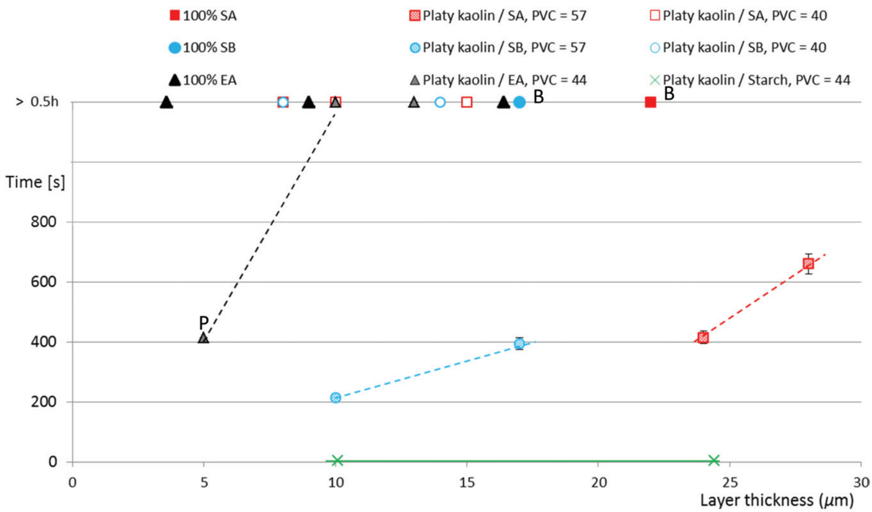

Figure 7. Barrier properties against 1 M hydrochloric acid. The figure shows the time in seconds for the liquid to penetrate the substrate. (B = Tendency for blocking, P = risk for pinholes). Penetration time measured with prism method presented in Figure 2B [50].

by the hydrochloric acid. Both the DCB and the hydrochloric acid penetrate the basepaper (including precoating and smoothing layer) in less than 5 seconds.

The binder, whether it is latex or starch can be considered the most important material for creating a sealed layer, but addition of mineral pigments can both improve the barrier properties as well as ensure problem free runnability and rewinding. Latexes, especially with low glass transition temperatures, tend to cause blocking problems, i.e. undesired adhesion of coating layer to the back of the adjacent paper in a roll, but addition of mineral pigment can significantly reduce the blocking problem.

3.3 Functional printability and surface properties

The ability to print narrow and well defined lines or structures is important, especially when high resolution devices are produced. In addition to the high requirements regarding line definition, functional printing also sets further demands regarding the actual functionality of the printed material, which usually is measured as electrical conductivity. Resistance is normally measured, which can be converted to conductivity. Since exact thicknesses and thereby volume resistivities are practically impossible to measure accurately on absorbing surfaces, surface resistivity (Ω/sq) was chosen as the main parameter for evaluating conductivity. In the multilayer coating structure it is the top-coating that determines the printability of the functional inks. Important coating layer properties affecting printability of functional inks are thickness, porosity, pore volume, surface energy and roughness. These can be adjusted by the choice of pigment shape, size and their distributions as well as by calendering [29, 37].

Conducting silver was printed both with flexography (roll-to-roll) and inkjet (batch). Two different silver inks were used, one consisting of flaky micrometer sized particles with a propylene glycol monomethyl ether acetate (PM acetate) as solvent designed for flexography and one containing nano sized particles with ethylene glycol as solvent designed for inkjet. As can be seen in the SEM image (Figure 8A), the nanoparticles of the silver ink penetrate into the pores of the silica coating rendering it nonconductive, but stay on the surface of both the kaolin and the kaolin/precipitated calcium carbonate (PCC) blend top-coatings. The pore volume of the top-coating was measured by mercury porosimetry [56, 57, 58, 59]. Since it is not possible to measure reliably the porosity of only the top-coating of a multilayer coated structure, pressure-filtrated tablets of the top-coating formulations were measured instead. With the knowledge of the porosity and the coat weight of the top-coating, the pore volume in the top-coating could then be estimated. The penetration of ink particles correlates with the top-coating dominant pore size, which for the kaolin and kaolin/PCC coatings was in the range of 13 to 80 nm and ca 380 nm for the silica coatings. The large pore size is a consequence of the relatively large particle size of the silica pigments used. The flexographic silver ink with micrometer sized flaky particles remained on the surface on all the top-coatings, and is thereby less sensitive to pore size (Figure 8B). A higher porosity and total available pore volume in the top-coating in fact allowed for faster ink vehicle uptake and thereby reduced the squeeze

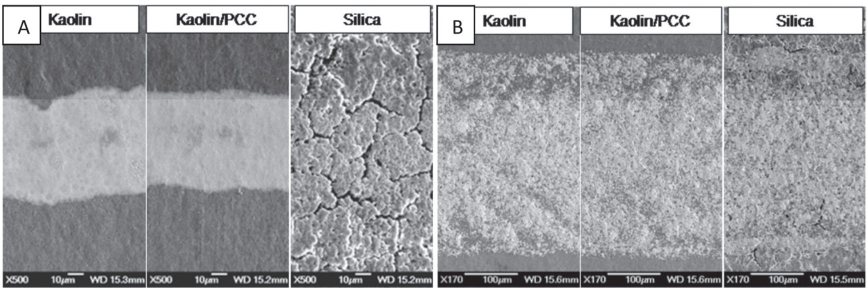

Figure 8. SEM images of silver particle inks printed with inkjet (A) and flexography (B) (3 g/m² top-coating). Reproduced with permission. Copyright 2012, Elsevier [29].

(ink spreading under printing nip pressure), improving the flexographic printability of micrometer sized particle ink [29].

Semiconductor, regioregular poly(3-hexylthiophene) (P3HT) dissolved in a mixture (1:1:2) of xylene:chlorobenzene:ortho-dichlorobenzene, was printed with inkjet at a solids content of 0.25 weight -%. The low solids content means a large amount of solvent is applied which has to evaporate or absorb into the coating structure. The solvent mixture vapor pressure was chosen to provide an evaporation rate, which is slow enough to eliminate clogging of the printing nozzles but fast enough to be printed in a roll-to-roll process. Too fast evaporation of the ink solvent leads to viscosity increase and deposits in the inkjet nozzle, where as too slow drying requires either slowing down of the roll-to-roll printing process or use of additional driers. However, excessive drying can potentially render the printed

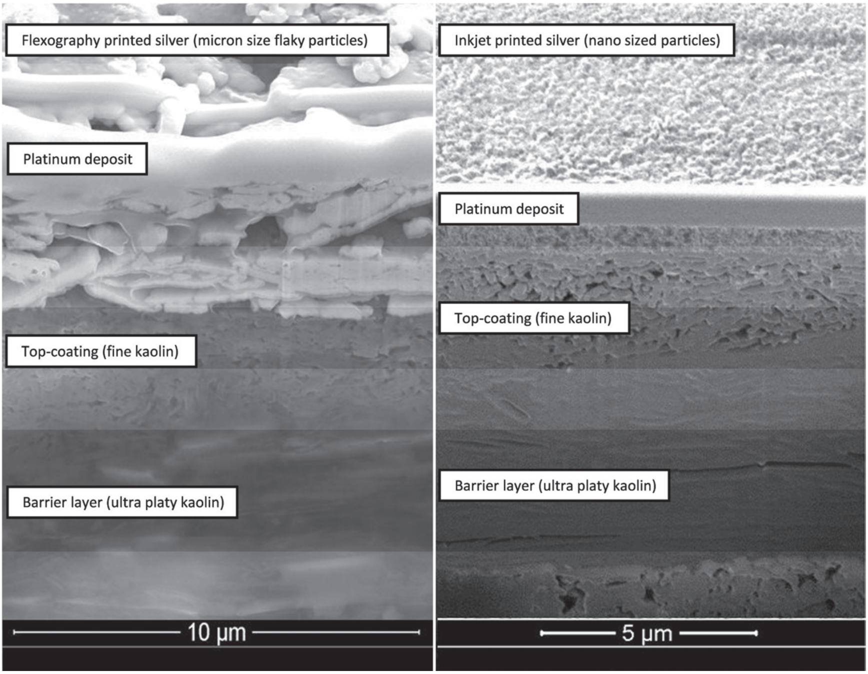

Figure 9. Focused ion beam cut and imaged cross-section of the coated paper substrate, showing flexography printed micrometer sized silver (LEFT) and inkjet printed nanoparticle silver (RIGHT) on the multilayer coating structure. The sectioned layers in the multilayer structure are, from the top: top-coating (5 g/m^2 fine kaolin), the barrier layer (10 g/m^2 platy kaolin) and the basepaper coating. The platinum deposit is required for the milling (ion beam cutting) through the coating structure.

device inoperable, e.g. due to crack propagation or a too high temperature destroy the semiconductive polymer. Semiconductor ink was printed at three different amounts, giving equal theoretical uniform dry thicknesses of 20 nm, 40 nm and 80 nm. This corresponds to applied P3HT-volumes of 2, 4 and 8 nl/cm^2 and to total printed volumes of 800, 1600 and 3200 nl/cm^2 respectively. These volumes were compared to the pore volumes in the top-coatings, which were in the range of 4 to 400 nl/cm^2.

All printed amounts on all the surfaces gave a visibly purple color, with darker color intensity for the higher amounts. Visually evaluated the most even films were achieved for the thinnest printed amounts (2 nl/cm^2) whereas the larger printed amounts (4 and 8 nl/cm^2) resulted in slow and uneven drying. Especially the substrates with low pore volume, and thereby limited absorptivity, exhibited coffee stain effect. Surface resistivity was measured for all the printed amounts and was correlated with the pore volume. As is shown in Figure 10, the relationship between the surface resistivity and the pore volume is almost linear for the small pore volumes (< 100 nl/cm^2) and the small amount of semiconductor (2 nl/cm^2). The impact of pore volume decreases as higher amounts of ink is applied. It is likely that for small applied ink volumes the semiconductor penetrates fully into the coating structure and surrounds the mineral particles, thereby creating a connecting network. Once the pores are filled, with both semiconductor and evaporating solvent, the rest of the applied amount will be on the surface and continued evaporation leads to an irregular film.

3.4 Dimensional stability

Dimensional stability was analysed by exposing substrates to humidity cycling. As reference substrates to the multilayer curtain coated (MLCC) paper, commercially available standard copy paper, double coated fine paper and a high quality

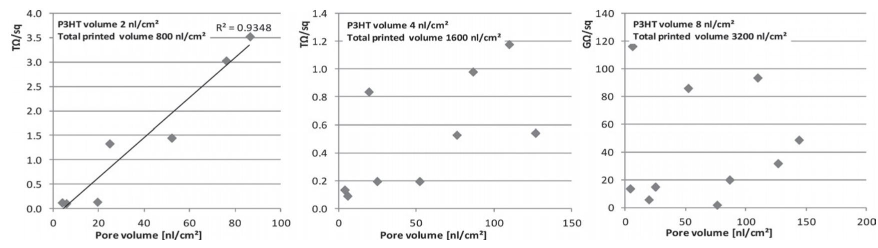

Figure 10. Surface resistivity as function of pore volume for 2 nl/cm^2 (left), 4 nl/cm^2 (middle) and 8 nl/cm^2 (right) total printed (roll-to-roll) semiconductor amounts. Reproduced with permission. Copyright 2012, Elsevier [29].

photo paper were tested. Silver lines (20 mm by ~100 µm, non-sintered) were inkjet printed onto the substrates at 23ºC and a relative humidity of 30%. The substrates with the printed lines were then stored for 24 hours in 90% relative humidity at 23ºC, then dried in a 100ºC oven for 30 minutes where after again stored in 90% relative humidity at 23ºC for 24 hours. Finally the substrates were stored in room conditions at 30% relative humidity at 23ºC for two days (Figure 11). The printed lines were scanned after each stage with a high resolution (6400 dpi) scanner and the exact line lengths were measured using image analysis to determine the expansion/shrinkage in x/y-plane. The measurement accuracy is ± 1 pixel equaling ± 4µm or 0.02%. Exposing the substrates to the first increased humidity level led to 0.1–0.3% expansion of all the substrates except for the inkjet paper which has a polymer film coating. Subsequent drying in oven shrank all the substrates by 0.35–0.6%, with smallest shrinkage observed for the MLCC paper and highest for the double coated fine paper. The polymer coated inkjet paper did not fully withstand the high temperature which resulted in permanent cracks in the polymer film. The second humidity level increase resulted in approximately the same dimensional changes as the first one, with the exception of the damaged inkjet paper. Overall, the dimensional changes were largest for the fine paper and copy paper. Compared to similar measurements of different nanocellulose based sheets conducted by Torvinen et al. [22], the dimensional changes observed here were in the same range. The multilayer coated substrate, including the strong barrier layer both limiting penetration and strengthening the structure of the

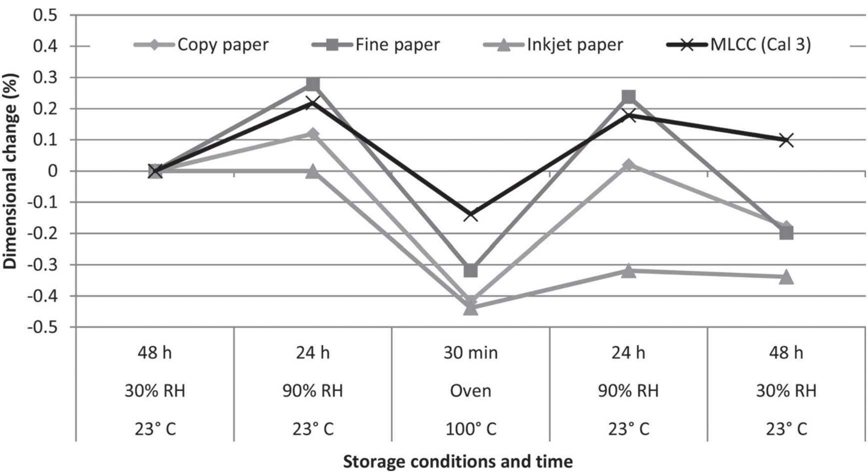

Figure 11. Dimensional change as function of humidity and temperature cycling for the different papers. Measurements are made after indicated time periods at each condition [37].

substrate showed small dimensional changes. Since the MLCC paper had the multilayer coating only on one side, this asymmetry led to curl of the paper. The curl can potentially be reduced or eliminated by coating the backside of the paper as well.

The changes in surface roughness of the double coated fine paper and MLCC caused by exposure of paper to high humidity were measured both by atomic force microscopy (AFM) and Parker Print-Surf (PPS) (1.0 MPa, soft backing). PPS allowed for fast measuring as a function of "drying" (90% RH → 50% RH @ 23ºC) after the samples had been brought into equilibrium at high humidity. After the samples were removed from the high humidity conditions, the PPS surface roughness increased slightly during the first 15 minutes. For MLCC the change was from 0.53 to 0.60 µm and for Fine paper from 0.87 to 1.05 µm (standard deviation ±0.03µm; values below 0.60 µm outside the ISO standard for PPS). This is potentially due to contraction of the fibers, which causes shrinkage of the basepaper fiber network. The initial surface roughness increase was observed for both the fine paper and the MLCC, but after the 15 minutes no change in roughness was detected for either one. Changes in surface roughness as a function of length scale were further studied by AFM (Figure 12A). Since obtaining an AFM image takes approximately one hour, the samples were stored for one hour in room conditions (25% RH and 23ºC) before starting the measurement, in order to avoid possible roughness change during the image acquisition. As can be seen in Figure 12A, the increase in roughness

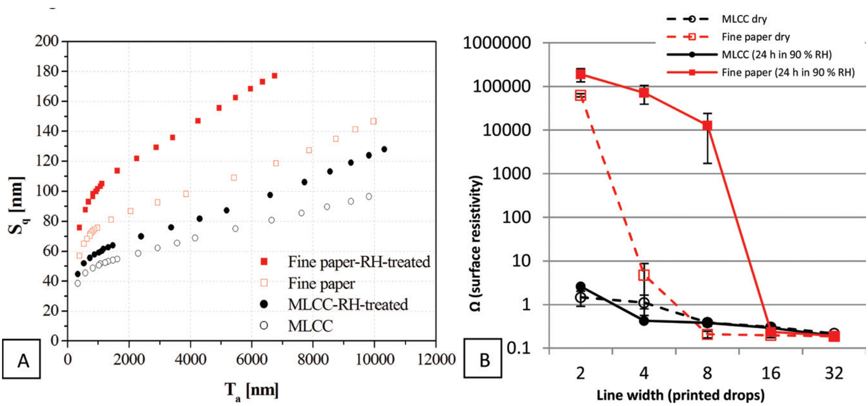

Figure 12. A: Root mean square roughness (S_q) as a function of correlation length (T_a), for MLCC and double coated fine paper before and after humidity treatment (24 h in 23ºC and 90% RH) [37]. B: Surface resistivity for different width printed silver tracks before and after humidity treatment.

is obvious on every length scale for the fine paper whereas it is significantly smaller for the multilayer curtain coated paper. For the fine paper the changes in surface roughness increase at longer length scales. This indicates the increase is a result of fiber swelling, since the roughness at longer length scales is determined by the base paper fibers [60, 61, 62]. Despite fiber swelling, which caused curl of the multilayer coated substrate, the mechanically strong barrier layer ensured that only minimal topographical changes on the coated side occurred.

The influence of humidity on conductivity was investigated by exposing printed silver tracks, with different line widths (2–32 inkjet printed 10 pl drops, drop spacing 20 μm), to humidity cycling. Surface resistivity was measured for the lines as they were printed and sintered (25% relative humidity) and again after 24 hour exposure to 90% relative humidity. As shown in figure 12B, the conductivity of the narrow printed tracks on the double coated fine paper, which showed the largest dimensional and surface roughness changes when exposed to high humidity, decreased considerably. The surface resistivity increased by 4 orders of magnitude for line widths printed with 4 and 8 drops. The impact on conductivity of the wider lines, printed with 16 and 32 drops, was negligible. On the multilayer coated paper, only a minimal impact on conductivity could be observed after the humidity treatment on the thinner lines (2 and 4 drops). No changes could be observed for the wider lines (8–32 drops). It is obvious that poor dimensional stability and roughening caused by humidity changes in the environment are detrimental to the functioning of narrow printed conductive tracks. In addition to the roughness increase and expansion of the substrate, oxidation of the silver particles might also play a role in slightly reducing the conductivity. Similar reduction in conductivity as function of treatment in high humidity conditions was also reported for printed tracks on different label papers by Wood et al. [63].

3.5 Proof-of-concept device

Several electronic devices and sensors have been successfully manufactured on the multilayer coated paper presented herein [16]. A hygroscopic insulator field effect transistor (HIFET) [64, 65] printed with a roll-to-roll hybrid printer serves as an example here. Figure 13A shows a schematic image of the top gate bottom contact field effect transistor geometry and an optical top view image of the gate electrode in blue, printed on top of a transparent insulator layer. Underneath is the purple semiconductor printed on top of silver electrodes. The output and transfer characteristics of the transistor are shown in Figure 13B and C, respectively. Compared to transistors manufactured in a batch process, especially on plastic substrates, the current throughput is rather low. Poor semiconductor

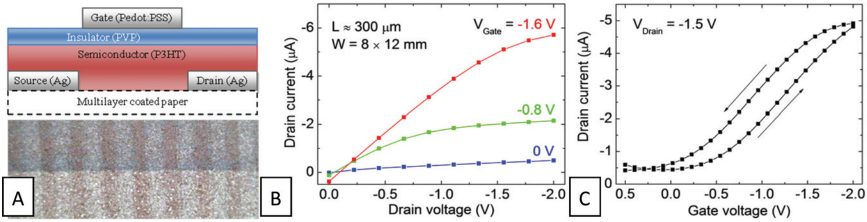

Figure 13. A: Schematic and optical image of a roll-to-roll printed HIFET. Output (B) and transfer (C) characteristics of the transistor on the multilayer curtain coated paper. Reproduced with permission. Copyright 2012, Elsevier [29].

ordering and impurities of the paper surface might degrade the charge transport [66, 67, 68].

4 CONCLUDING REMARKS

The understanding of the interactions between functional materials formulated and applied on paper as inks, makes it possible to create a paper-based substrate that can be used to manufacture printed electronics-based devices and sensors on paper. The multitude of functional materials and their complex interactions make it challenging to draw general conclusions in this topic area. The results become partially specific to the device chosen and the materials needed in its manufacturing. Based on the results, it is clear that for inks based on dissolved or small size functional materials, a barrier layer is essential and ensures the functionality of the printed material in a device. The required active barrier life time depends on the solvents or analytes used and their volatility. High aspect ratio mineral pigments, which create tortuous pathways and physical barriers within the barrier layer limit the penetration of solvents used in functional inks. The surface pore volume and pore size can be optimized for a given printing process and ink through a choice of pigment type and coating layer thickness. However, when manufacturing multilayer functional devices, such as transistors, which consist of several printed layers, compromises have to be made. E.g., while a thick and porous top-coating is preferable for printing of source and drain electrodes with a silver particle ink, a thinner and less absorbing surface is required to form a functional semiconducting layer. The possibility of printing transistors in a roll-to-roll process on paper is demonstrated. For industrial production of the paper for printed electronics, curtain coating is a suitable coating technique allowing extremely thin top-coatings to be applied simultaneously with a closed and sealed barrier layer.

5 ACKNOWLEDGEMENTS

This article is a compilation of several separately published articles. The authors want to acknowledge Anni Määttänen, Daniel Tobjörk, Peter Dolietis, Roger Nyqvist, Jarkko J Saarinen, Petri Ihalainen, Janet Preston, Pekka Salminen, Jouko Peltonen and Ronald Österbacka for their contribution in development and analyses of the multilayer coating structure. Imerys Minerals Ltd., Styron Europe GmbH, Specialty Minerals Nordic Oy, Paramelt B.V., StoraEnso, and Basf are acknowledged for providing materials. Academy of Finland (Grant 118650) and Tekes (Grant 40092/09) are acknowledged for financial support.

6 REFERENCES

1. D. Tobjörk and R. Österbacka, "Paper Electronics," *Adv. Mater.*, vol. 23, pp. 1935–1961, 2011.
2. P. Przybysz, "E-paper-potential competitor and printing papers," *Forestry Wood Technol.*, vol. 59, pp. 210–213, 2006.
3. N. Robinson and M. Berggren, "Printing organic electronics on flexible substrates," in *Handbook of Conducting Polymers, Conjugated Polymers: Processing Applications*, 3rd ed., T. Francis, Ed., New York, 2007, pp. 4–1–4–26.
4. B. Trnovec, M. Stanel, U. Hahn, A. Huebler, H. Kempa and R. Sangl, "Coated paper for printed electronics," *Professional Papermaking*, pp. 48–51, 2009.
5. A. Siegel, S. Phillips, B. Wiley and G. Whitesides, "Thin, lightweight, foldable thermochromic displays on paper," *Lab Chip*, vol. 9, pp. 2775–2781, 2009.
6. M. Pudas, N. Halonen, P. Granat and J. Vähäkangas, "Gravure printing of conductive particulate polymer inks on," *Prog. Org. Coat.*, vol. 54, pp. 310–316, 2005.
7. M. Dragoman, E. Flahaut, D. Dragoman, M. Ahmad and R. Plana, "Writing simple RF electronic devices on paper with carbon nanotube ink," *Nanotechnology*, vol. 20, p. 375203, 2009.
8. B. Lamprecht, R. Thunauer, M. Ostermann, G. Jakopic and G. Leising, "Organic photodiodes on newspaper," *Phys. Status Solidi A*, vol. 202, pp. 50–52, 2005.
9. J. Shah and R. Brown Jr, "Towards electronic paper displays made from microbial cellulose," *Appl. Microbiol. Biotechnil.*, vol. 66, pp. 352–355, 2005.
10. K. Braam, S. Volkman and V. Subramanian, "Characterization and optimization of a printed, primary silver–zinc battery," *Journal of Power Sources*, 2011.
11. M. Hilder, N. Winther-Jensen and N. Clark, "Paper-based, printed zinc–air battery," *Journal of Power Sources*, vol. 194, pp. 1135–1141, 2009.
12. Y. Kim, D. Moon and J. Han, "Organic TFT array on a paper substrate," *IEEE Electron Device Lett.*, vol. 25, pp. 702–704, 2004.
13. P. Andersson, R. Forchheimer, P. Tehrani and M. Berggren, "Printable all-organic electrochromic active-matrix displays," *Adv. Funct. Mater*, vol. 17, pp. 3074–3082, 2007.

14. A. Huebler, B. Trnovec, T. Zillger, M. Ali, N. Wetzold, M. Mingebach, A. Wagenpfahl, C. Deibel and V. Dyakonov, "Printed Paper Photovoltaic Cells," *Adv. Energy Mater.*, 2011.
15. M. Barr, J. Rowehl, R. Lunt, J. Xu, A. Wang, C. Boyce, G. Im Sung and V. G. K. Bulovic, "Direct Monolithic Integration of Organic Photovoltaic Circuits on Unmodified Paper," *Adv. Mater.*, vol. 23, pp. 3500–3505, 2011.
16. R. Bollström, D. Tobjörk, P. Dolietis, T. Remonen, C.-J. Wikman, S. Viljanen, J. Sarfraz, P. Salminen, M. Lindén, C.-E. Wilén, J. Bobacka, R. Österbacka and M. Toivakka, "Roll-to-roll printed electronics on paper," in *Proceedings of TAPPI PaperCon 2012*, New Orleans, 2012.
17. A. Määttänen, D. Fors, S. Wang, D. Valtakari, P. Ihalainen and J. Peltonen, "Paper-Based Planar Reaction Arrays for Printed Diagnostics," *Sens. Actuators B*, vol. 160, p. 1404, 2011.
18. J. Sarfraz, D. Tobjörk, R. Österbacka and M. Lindén, "Low-Cost Hydrogen Sulfide Gas Sensor on Paper Substrates: Fabrication and Demonstration," *IEEE Sensors Journal*, vol. 12, no. 6, 2012.
19. J. Olkkonen, K. Lehtinen and T. Erho, "Flexographically Printed Fluidic Structures in Paper," *Anal. Chem.*, vol. 82, pp. 10246–10250, 2010.
20. A. Martinez, S. Phillips, G. Whitesides and E. Carrilho, "Diagnostics for the Developing World: Microfluidic Paper-Based Analytical Devices," *Anal. Chem.*, vol. 82, no. 3, 2010.
21. R. Pelton, "Bioactive Paper Provides a Low-Cost Platform for Diagnostics," *Anal. Chem*, vol. 28, p. 925, 2009.
22. K. Torvinen, J. Sievänen, T. Hjelt and E. Hellén, "Smooth and flexible filler-nanocellulose composite structure for printed electronics applications," *Cellulose*, vol. 19, pp. 821–829, 2012.
23. M. Cruz, M. Joyce, P. Fleming, M. Rebros and A. Pekarovicova, "Surface Topography Contribution to RFID Tag Efficiency Related To Conductivity," in *TAPPI Coating and Graphic Arts*, Miami, 2007.
24. R. Kattumenu, M. Rebros, M. Joyce, P. Fleming and G. Neelgund, "Effect of substrate properties on conductive traces printed with silver-based flexographic ink," *Nord. Pulp Pap Res J*, vol. 24, pp. 101–106, 2009.
25. P. Ihalainen, A. Määttänen, J. Järnström, D. Tobjörk, R. Österbacka and J. Peltonen, "Influence of Surface Properties of Coated Papers on Printed Electronics," *Ind. Eng. Chem. Res.*, vol. 51, pp. 6025–6036, 2012.
26. A. Määttänen, P. Ihalainen, R. Bollström, M. Toivakka and J. Peltonen, "Wetting and print quality study of an inkjet-printed poly(3-hexylthiophene) on pigment coated papers," *Colloids Surf. A: Physicochem. Eng. Aspects*, vol. 367, pp. 76–84, 2010.
27. E. Hrehorova, A. Pekarovicova, V. Bliznyuk and P. Fleming, "Polymeric Materials for Printed Electronics and Their Interactions with Paper Substrates," in *IS&T Digital Fabrication*, Anchorage, 2007.
28. E. Hrehorova, A. Pekarovicova and P. Fleming, "Evaluation of Gravure Printing for Printed Electronics," in *Technical Assosiation of the Graphic Arts (TAGA)*, San Fransisco, 2008.

29. R. Bollström, D. Tobjörk, P. Dolietis, P. Salminen, J. Preston, R. Österbacka and D. Toivakka, “Printability of functional inks on multilayer curtain coated paper,” *Chemical Engineering and Processing*, vol. 68, pp. 13–20, 2013.
30. T. Uesaka, “Dimensional stability of paper. Upgrading paper performance in end use,” *Journal of Pulp and Paper Science*, vol. 17, no. 2, pp. 39–46, 1991.
31. K. Schulgasser, “Moisture and thermal expansion of wood, particleboard and paper,” *Paperi ja Puu*, vol. 70, no. 6, pp. 534–539, 1988.
32. C. Green, “Dimensional Properties of Paper Structures,” *Ind. Eng. Chem. Prod. res. Dev.*, vol. 1081, no. 20, pp. 151–158, 1981.
33. T. Schuman, M. Wikström and M. Rigdahl, “Dispersion coating with carboxylated and cross-linked styrene–butadiene lattices 2. Effects of substrate and polymer characteristics on the properties of coated paperboard,” *Prog. Org. Coat.*, vol. 51, p. 228, 2004.
34. T. Schuman, A. Karlsson, J. Larsson and M. Wikström, “Characteristics of pigment-filled polymer coatings on paperboard,” *Prog. Org. Coat.*, vol. 54, pp. 360–371, 2005.
35. R. Bollström, R. Nyqvist, J. Preston, P. Salminen and M. Toivakka, “Barrier properties created by dispersion coating,” *TAPPI Journal*, vol. (In Press), 2013.
36. R. Bollström, A. Määttänen, D. Tobjörk, P. Ihalainen, N. Kaihovirta, R. Österbacka, J. Peltonen and M. Toivakka, “A multilayer coated fiber-based substrate suitable for printed functionality,” *Org. Electron.*, vol. 10, pp. 1020–1023, 2009.
37. R. Bollström, F. Pettersson, P. Dolietis, J. Preston, R. Österbacka and M. Toivakka, “Impact of humidity on functionality of on-paper printed electronics,” *Submitted 2013*.
38. R. Bollström, M. Tuominen, A. Määttänen, J. Peltonen and M. Toivakka, “Top layer coatability on barrier coatings,” *Progress in Organic Coatings*, vol. 73, pp. 26–32, 2012.
39. R. Bollström, A. Määttänen, P. Ihalainen, J. Peltonen and M. Toivakka, “Method for creating a substrate for printed or coated functionality, substrate, functional device and its use”. Patent PCT/FI2010/050056, WO2010/086511, 2009.
40. D. Tobjörk, H. Aarnio, P. Pulkkinen, R. Bollström, P. Ihalainen, T. Mäkelä, J. Peltonen, M. Toivakka, H. Tenhu and R. Österbacka, “IR-sintering of ink-jet printed metal-nanoparticles on paper,” *Thin Solid Films*, vol. 520, no. 7, pp. 2949–2955, 2012.
41. G. Gugler, R. Beer and M. Mauron, “Operative limits of curtain coating due to edge,” *Chemical Engineering and Processing*, vol. 50, pp. 462–465, 2011.
42. S. Renvall, T. Nurmiainen, J. Haavisto, I. Endres, R. Urscheler and K. Tano, “New cost-efficient concept for coated white top liner with on-machine multilayer curtain coating,” in *Kami Parupu Gijutsu Kyokai, General Review*, CODEN:NTKKFN, 2009, pp. 276–280.
43. T. Lamminmäki, J. Kettle, H. Rautkoski, A. Kokko and P. Gane, “Limitations of Current Formulations when Decreasing the Coating Layer Thickness of Papers for Inkjet Printing,” *Ind. Eng. Chem. Res.*, vol. 50, pp. 7251–7263, 2011.
44. G. Haya, D. Southee, P. Evans, D. Harrison, G. Simpson and B. Ramsey, “Examination of silver-grafite lithographically printed resistive strain sensors,” *Sensor and Actuatiors A*, vol. 135, pp. 534–546, 2007.

45. M. O'Toolea, R. Shepherd, G. Wallace and D. Diamond, "Inkjet printed LED based pH chemical sensor for gas sensing," *Analytica Chimica Acta*, vol. 652, pp. 308–314, 2009.
46. N. Martinez, G. Messina, F. Bertolina, E. Salinas and J. Raba, "Screen-printed enzymatic biosensor modified with carbon nanotube for the methimazole determination in pharmaceuticals formulations," *Sensors and Actuators B*, vol. 133, pp. 256–262, 2008.
47. D. Nilson, T. Kugler, P. Svensson and M. Berggren, "An all-organic sensor transistor based on a novel electrochemical transducer concept printed electrochemical sensors printed on paper," *Sensors and Actuators B*, vol. 86, pp. 193–197, 2002.
48. S. Anastasova, A. Radu, G. Matzeu, C. Zuliani, D. Diamond, U. Mattinen and J. Bobacka, "Disposable solid-contact ion-selective electrodes for environmental monitoring of lead with ppb limit-of-detection," *Electrochim Acta*, vol. 73, no. 1, p. 93, 2012.
49. J. J. Saarinen, P. Ihalainen, A. Määttänen, R. Bollström and J. Peltonen, "Printed sensor and electric field assisted wetting on a natural fibre based substrate," *Nordic Pulp And Paper Research Journal*, vol. 26, no. 1, p. 133, 2011.
50. R. Bollström, J. J. Saarinen, J. Räty and M. Toivakka, "Measuring solvent barrier properties of paper," *Meas. Sci. Technol.*, vol. 23, p. 015601, 2012.
51. R. Colvin, "Environmentally friendly barrier coating moves to packaging," *Mod. Plastics*, vol. 33, no. 13, p. 29, 2003.
52. C. Andersson, M. Ernström and L. Järnström, "Barrier preoperties and heat sealability/failure mechanisms of dispersion-coated paperboard," *Packag. Technol. Sci.*, vol. 15, p. 209, 2002.
53. D. Perera, "Effect of pigmentation on organic coating characteristics," *Progress in Organic Coatings*, vol. 50, pp. 247–262, 2004.
54. G. del Rio and A. Rudin, "Latex particle size and CPVC," *Progress in Organic Coatings*, vol. 28, pp. 259–270, 1995.
55. J. Preston, C. Nutbeem and R. Chapman, "Impact of Pigment Blend and Binder Level on the Structure and Printability of Coated Papers," in *Tappi PaperCon*, Cincinnati, 2011.
56. C. Gribble, G. Matthews, G. Laudone, A. Turner, C. Ridgway, J. Schoelkopf and P. Gane, "Porometry, porosimetry, image analysis and void network modelling in the study of the pore-level properties of filters," *Chem. Eng. Sci.*, vol. 66, pp. 3701–3709, 2011.
57. C. Ridgway, P. Gane and J. Schoelkopf, "Effect of Capillary Element Aspect Ratio on the Dynamic Imbibition within Porous Networks," *J. Colloid Interface Sci.*, vol. 252, p. 373, 2002.
58. C. Ridgway and P. Gane, "Controlling the Absorption Dynamic of Water-Based Ink into Porous Pigmented Coating Structures to Enhance Print Performance," *Nord. Pulp Pap. Res. J.*, vol. 17, p. 119, 2002.
59. R. Olsson, J. van Stam and M. Lestelius, "Effects on Ink Setting in Flexographic Printing: Coating Polarity and Dot Gain," *Nord. pulp Pap. Res. J.*, vol. 21, p. 569, 2006.

60. J. Järnström, L. Sinervo, M. Toivakka and J. Peltonen, "Topography and gloss of precipitated calcium carbonate coating layers on a model substrate," *Tappi Journal*, vol. 6, p. 23, 2006.
61. J. Järnström, P. Ihalainen, K. Backfolk and J. Peltonen, "Roughness of pigment coatings and its influence on gloss," *Applied Surf. Sci*, vol. 254, p. 5741, 2008.
62. S. Wang, P. Ihalainen, J. Järnström and J. Peltonen, "The effect of base paper and coating method on the surface roughness of pigment coatings," *J. Disp. Sci. and Tech.*, vol. 30, p. 961, 2009.
63. L. Wood, T. Joyce, P. Fleming and M. Joyce, Paper Substrates and Inks for Printed Electronics, Atlanta: Pira Ink on Paper Symposium, 2005.
64. H. Sandberg, T. Bäcklund, R. Österbacka and H. Stubb, "A high performance all-polymer transistor utilizing a hygroscopic insulator," *Adv. Mater.*, vol. 16, pp. 1112–1115, 2004.
65. D. Tobjörk, N. Kaihovirta, T. Mäkelä, F. Pettersson and R. Österbacka, "All-printed low-voltage organic transistors," *Org. Electron.*, vol. 9, pp. 931–935, 2008.
66. D. Tobjörk, R. Bollström, P. Dolietis, A. Määttänen, P. Ihalainen, T. Mäkelä, J. Peltonen, M. Toivakka and R. Österbacka, "Printed low-voltage organic transistors on plastic and paper," in *European Coating Symposium*, Turku, 2011.
67. R. Bollström, D. Tobjörk, A. Määttänen, P. Ihalainen, J. Peltonen, R. Österbacka and M. Toivakka, "Towards Paper Electronics- Printing Transistors on Paper in a Roll-To-Roll Process," in *NIP 27 and Digital Fabrication*, Minneapolis, 2011.
68. D. Tobjörk, Printed Low-Voltage Organic Transistors on Plastic and Paper, PhD Thesis, Turku: Åbo Akademi University, 2012.

Transcription of Discussion

PAPER SUBSTRATE FOR PRINTED FUNCTIONALITY

Roger Bollström and Martti Toivakka

Laboratory of Paper Coating and Converting, Centre for Functional Materials
Åbo Akademi University

Li Yang Innventia

Thank you for a very nice presentation. I have a few questions, the first is what kind of inkjet printer did you use?

Roger Bollström

We use two types of inkjet printer: we have a Dimatix™ for batch printing, and we also have one we built ourselves based on Xaar's printheads for the roll-to-roll printer. We have printheads with 10 pL drop volume for the Dimatix printer, and we have 40 pL and 80 pL for the Xaar setup.

Li Yang

Which one is better from the performance point of view?

Roger Bollström

Well, of course you get higher resolution with the Dimatix, with the smaller droplet size. When I, for example, compared printing the semiconductor, I got similar results, but it also depends on other factors. It is very slow to print in batch mode.

Li Yang

In one slide, you show the line width, in terms of number of droplets. Which printer was it because it makes a big difference?

Roger Bollström

That was with the Dimatix.

Li Yang

You demonstrate how you improve the coating in order to improve the printability. In practice, because you are not printing in one layer, you print a few layers – for example, you printed semiconductor, insulator and silver – the printer is an issue as well. Can you say something more on that?

Roger Bollström

Yes, maybe the best example here is the transistor. In this case, both the silver electrodes and the semiconductor come into contact with the coating structure directly, then there is the insulator layer that is printed on top of these, so, for that, the paper properties do not have any effect, but quite often we need to compromise.

Li Yang

That is printed with inkjet or with flexography?

Roger Bollström

This has been printed with both the inkjet and flexography; the silver electrodes are flexographically printed at quite a large scale, but when we go to smaller, narrower channels in the transistor, then we go to inkjet.

Anders Åström Aylesford Newsprint (from the chair)

You talked about sustainability and recyclability, and of course, paper is a well established, recyclable product; how is its recyclability affected by printing electronics on it?

Roger Bollström

That is a very good question. Well, silver I guess is a bit questionable regarding that, but the other inks are all organic materials. I do not have a clear answer. The carbon again should not be a problem. It depends on the application and what material you use, and that definitely is something that has to be taken into account.

Andreas Kornherr Mondi

Could you comment on the curing temperature for the silver inks, and on the conductivity you can achieve?

Roger Bollström

Yes, but actually it is not just curing, there is also a sintering process. We use infrared sintering for that. I actually forgot to mention that the use of paper or coated paper is also extremely advantageous because it can withstand the high temperatures. If I printed the same thing on plastic, I would not be able to use these high temperatures, and that means a long time is then required. When we print roll-to-roll at, for example, 10 metres per minute, using infrared drying and sintering, it is sufficient to give us the conductivity we need.

Andreas Kornherr

And the maximum conductivity, compared to the bulk conductivity of silver, and the percentages? What can you achieve?

Roger Bollström

Measuring the exact thickness is a bit difficult but I do not think that we reach the bulk conductivity, but we are not that far away from it.